An Upper Bound for the Tidally Rectified Current at One Location on the Southern Flank of Georges Bank

BRADFORD BUTMAN AND MARLENE NOBLE

United States Geological Survey, Woods Hole, MA 02543

DAVID C. CHAPMAN AND ROBERT C. BEARDSLEY

Woods Hole Oceanographic Institution[1], *Woods Hole, MA 02543*

(Manuscript received 20 April 1982, in final form 24 January 1983)

ABSTRACT

Long-term current observations at 45 and 75 m at one location on the southern flank of Georges Bank in water 85 m deep were examined for evidence of tidal rectification. Loder has shown analytically that rectification of the strong semidiurnal tidal current can cause a mean along-bank flow, and thus may partially drive the observed clockwise circulation around Georges Bank. The amplitude of the tidally rectified along-bank flow is proportional to the squared amplitude of the cross-bank tidal current. A simple extension of Loder's model to include the weaker N_2 and S_2 tidal components suggests that fortnightly (354 h) and monthly (661 h) variations of the square of the cross-bank tidal current should cause a modulation of the subtidal along-bank flow.The predicted ratio (R) of the fortnightly and monthly modulation of the along-bank flow to the mean along-bank flow on the southern flank was a function of position and ranged from ~0.1–0.5. The amplitude of modulation of the along-bank flow at 360 and 648 h, estimated from the (weak) coherence between the observed along-bank flow and the subtidal envelope of a simulated surface tide, was *less* than ~1.1 and 0.9 cm s^{-1}, respectively, at 45 m. The amplitude of the modulation which can be attributed to tidal rectification may be in error by the astronomically forced Mm and MSf tidal currents, which are undescribed in this region. However, the magnitude of the mean along-bank tidally rectified current determined from the observed modulation and R predicted by the analytical model was ~2.0 cm s^{-1} at 45 m (36% of the observed mean current in winter) and less than 1.6 cm s^{-1} at 75 m (43% of the observed mean current). Although R may change in a more realistic model, this analysis suggests that only part of the seasonal-mean along-bank flow on the southern flank of Georges Bank may be caused by tidal rectification.

1. Introduction

Georges Bank is a shallow submarine bank at the mouth of the Gulf of Maine. Recent direct current measurements have confirmed a clockwise circulation around the Bank (Butman *et al.*, 1982, Fig. 1). The observed currents were primarily parallel to the isobaths. Currents along the steep northern flank were approximately 20–35 cm s^{-1}, and were 5–10 cm s^{-1} along the broader southern flank. Loder (1980) and Hopkins and Garfield (1981) have suggested that rectification of the strong M_2 tidal current may partially drive the mean along-bank flow. Loder considered the mean along-bank flow driven by the semidiurnal tide and found that the amplitude of the along-bank flow was proportional to the square of the cross-bank tidal current amplitude. This suggests that spring–neap variations in the tidal forcing should cause spring–neap variations in the mean along-bank flow.

In this paper the spring–neap variations of the along-bank flow are used to estimate the portion of the mean along-bank flow caused by tidal rectification. A simple extension of Loder's model to include several semidiurnal tidal components (developed in the next section) indicates that the observed subtidal along-bank current should be coherent with the square of the total tidal current. The subtidal along-bank flow observed at one location on the southern flank of Georges Bank (where a very long data set has been collected) is examined for spring–neap modulation at fortnightly (354 h) and monthly (661 h) periods. The coherence between the observed subtidal along-bank current and the square of the total tidal current (or surface tide) is used to estimate the amplitude of the spring–neap modulation. The results of the analytical model are then used to estimate the amplitude of the mean along-bank current driven by tidal rectification.

[1] Woods Hole Oceanographic Institution Contribution No. 5366.

© 1983 American Meteorological Society

Unauthenticated | Downloaded 05/27/24 09:13 PM UTC

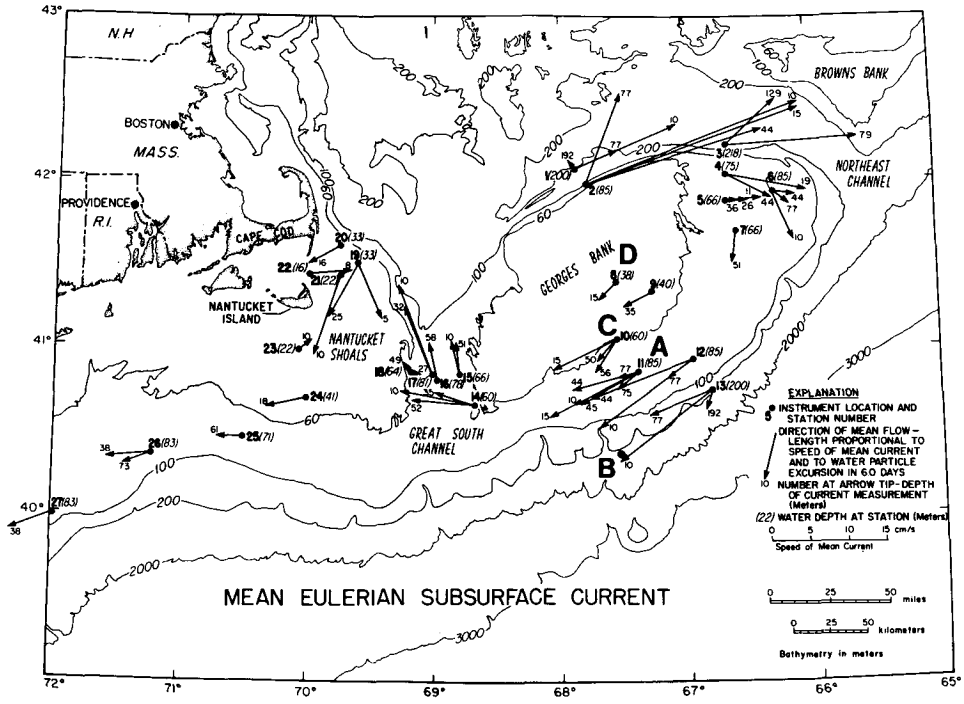

FIG. 1. Mean Eulerian subsurface currents on Georges Bank (from Butman *et al.*, 1982). The length of each vector is proportional to the mean current speed. The current measurements are not synoptic nor of equal duration, but were compiled from measurements of varying length (one month minimum) made at different times during the 4 year period 1975–79. Note the strong northeastward flow along the northern flank of Georges Bank and the weaker southwestward flow along the southern flank. The long-term observations of currents reported in this paper were made at station A (45 and 75 m) from August 1976 to March 1979. Currents were also measured for shorter periods at stations B, C, and D and pressure at stations A and C. Stations A, C, and D correspond to locations 11, 10, and 8, respectively in Fig. 1.

2. Conceptual model

Huthnance (1973) was the first to examine the mean along-bank flow driven by the Reynolds stress divergence associated with the propagation of a single tidal constituent onto a submarine bank. Assuming that the tidal currents were linearly polarized in deep water, Huthnance computed the mean along-bank flow due to the nonlinear interaction of the lowest-order tidal currents, ignoring both higher-order harmonic interaction and interaction between tidal and mean flows. Loder (1980) extended Huthnance's analysis to include spatially varying bottom friction, elliptic polarization of the tidal current in deep water, and mean flow interaction. In this paper, Huthnance's (1973) model is extended to include two semidiurnal tidal components, each linearly polarized in deep water, and the variable bottom friction used by Loder (1980). The model development closely parallels that of Loder (1980). Although the mean-flow interaction is ignored, the extended model is analytically simple and retains the essential physics of the rectification mechanism necessary to study the spring–neap variation in the subtidal along-bank flow.

The model topography is assumed two-dimensional; the positive y axis is aligned in the along-bank direction and the positive x axis points toward shallow water (Figure 2). Following Loder (1980), the velocities are assumed to be barotropic and independent of y, and there is no cross-isobath variation in the along-isobath sea-surface slope. The governing momentum equations are then

$$u_t + uu_x - fv = -g\zeta_x - \frac{ku}{h}, \tag{1a}$$

$$v_t + uv_x + fu = -g\zeta_y - \frac{kv}{h}, \tag{1b}$$

where $k(x)$ is the friction coefficient (discussed below) and $h(x)$ is the water depth. The cross-bank scale of the topography is considered to be small compared to the deep-water cross-bank wavelength of the tidal components, so that the flow is nondivergent in x, i.e.,

$$hu = \text{constant} = h_0u_0, \tag{2}$$

where the subscript zero designates the (constant) value of the variable in deep water.

Since the nonlinear effects are assumed to be insignificant in deep water, the sea-surface slope may

Unauthenticated | Downloaded 05/27/24 09:13 PM UTC

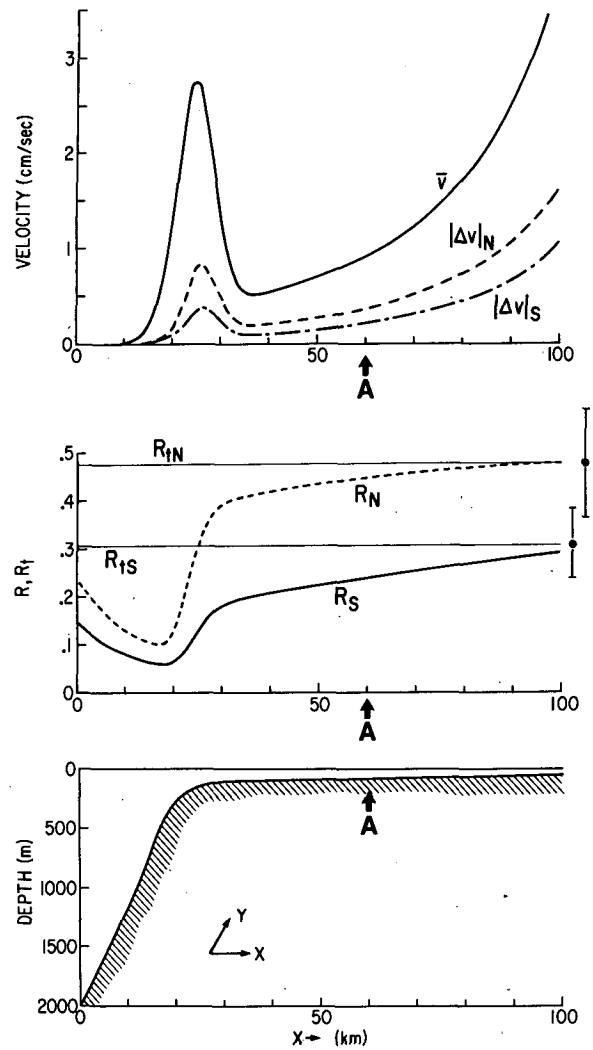

FIG. 2. (Upper panel) Mean flow $\bar{v}$ and the amplitudes of the fortnightly and monthly mean flow modulations, $|\Delta v|_S$ and $|\Delta v|_N$, predicted using the model parameters in Table 2. (Middle panel) Predicted fortnightly and monthly modulation ratios R_S and R_N given by (11) and the corresponding tidal modulation ratios, R_{tS} and R_{tN}, given by (13). Error bars show the standard deviation of the R_t estimates computed from the six mid-depth tidal current observations at stations A–D (Table 1). (Lower panel) Model topography corresponding to a transect through Station A.

be eliminated from (1b) by evaluating (1b) in deep water and subtracting that value from (1b) to yield

$$(v - v_0)_t + uv_x + f(u - u_0) = -\left(\frac{kv}{h} - \frac{k_0 v_0}{h_0}\right). \quad (3)$$

The time average of (3) is then

$$-k\bar{v} = h\overline{uv}_x, \quad (4)$$

where the overbar represents a time average over many tidal periods. Eq. (4) represents the principal balance for tidally rectified flow between the bottom drag on the mean along-bank flow and the divergence of the momentum flux (or Reynolds stress) associated with the tidal component. The lowest-order tidal currents are used to compute the right-hand side of (4).

We now consider the mean along-bank flow driven by the lowest-order interaction of two semidiurnal tidal components with frequencies σ_1 and σ_2. The velocity field can be decomposed into

$$v = \bar{v} + (\tfrac{1}{2}\Delta v e^{i\Delta\sigma t} + \tfrac{1}{2}\Delta v^* e^{-i\Delta\sigma t}) + \sum_{i=1}^{2} (\tfrac{1}{2}v_i e^{i\sigma_i t} + \tfrac{1}{2}v_i^* e^{-i\sigma_i t}) + \cdots, \quad (5a)$$

$$u = \sum_{i=1}^{2} (\tfrac{1}{2}u_i e^{i\sigma_i t} + \tfrac{1}{2}u_i^* e^{-i\sigma_i t}) + \cdots, \quad (5b)$$

where $\bar{v}$ is the mean along-bank current, $|\Delta v|$ is the amplitude of the low-frequency along-bank current which varies with frequency $\Delta\sigma = \sigma_1 - \sigma_2$, and where the subscripts 1 and 2 indicate the two semidiurnal tidal components (1 for M_2 and 2 for either N_2 or S_2). The asterisk designates the complex conjugate. Higher-order harmonic terms have been ignored. The terms $\bar{u}$ and Δu are also omitted in (5b) because of continuity (2) and the vanishing of any nonlinear effects in deep water. For simplicity, it is assumed that each tidal component is linearly polarized in deep water and aligned in the cross-bank direction (i.e., $v_{i0} = 0$).

To obtain explicit expressions for the mean $\bar{v}$ and the low-frequency variation $|\Delta v|$ in terms of bottom depth and the amplitude of the two tidal components, the momentum and continuity equations (1, 2, and 3) are separated into different frequency components and solved separately. [Note that because of the quadratic nonlinearity in (4), only two tidal components need be considered at once. The results of the pairs can then be superposed.] Following Loder (1980), the friction coefficient is assumed to be proportional to the cross-bank M_2 tidal velocity,

$$k(x) = C_D u_M,$$

where C_D is a drag coefficient and the subscript M designates the M_2 tidal component. Using (2) we obtain

$$k(x) = C_D h_0 u_{M0}/h. \quad (6)$$

Because the M_2 velocity on Georges Bank is much larger than either the mean flow or the N_2 or S_2 velocities, the friction coefficient is relatively independent of these other components. Therefore, Eq. (6) is appropriate for all tidal frequencies by an argument similar to that of Hunter (1975).

The lowest-order equations at the two tidal frequencies σ_1 and σ_2 can be solved (ignoring mean-flow interaction) to obtain

$$v_{ix} = u_{i0} h_x A_i, \quad (7)$$

Unauthenticated | Downloaded 05/27/24 09:13 PM UTC

where

$$A_i = \frac{f}{\sigma_i^2 h^2 (F_i^2 + 1)^2} \left\{ F_i^2 k \left(2 - \frac{h_0}{h} \right) + k \left(3 \frac{h_0}{h} - 2 \right) + i \left[F_i k \left(3 \frac{h_0}{h} - 4 \right) - \sigma_i h_0 \right] \right\},$$

and $F_i = k/(\sigma_i h)$ is the ratio of frictional to inertial forces. This result is identical to that obtained from Loder's equation (14) by setting $R = 0$ and differentiating with respect to x. The mean flow is then calculated by substituting (7) into (4) to obtain

$$\bar{v} = \frac{-h}{4k} \sum_{i=1}^{2} (u_i v_{ix}^* + u_i^* v_{ix}) = \frac{-1}{4k} \sum_{i=1}^{2} [h_0 |u_{i0}|^2 h_x (A_i + A_i^*)]. \quad (8)$$

The governing equation for the complex modulation at the difference frequency $\Delta\sigma$ is

$$(-k - ih\Delta\sigma)\Delta v = \tfrac{1}{2} h (u_1 v_{2x}^* + u_2^* v_{1x}). \quad (9)$$

Note that in shallow water where h is small, the dynamical balance for the modulation is essentially the same as that for the mean flow in (4). However, in deep water, the balance may be different because the inertial acceleration (which is absent for the mean flow) may become important in (9). The magnitude of the complex modulation is given by

$$|\Delta v| = \frac{h_0 |u_{10}| |u_{20}| h_x}{2(\Delta\sigma^2 h^2 + k^2)^{1/2}} \times (A_1 A_1^* + A_1 A_2 + A_1^* A_2^* + A_2 A_2^*)^{1/2}. \quad (10)$$

Thus the complex modulation of the along-bank current at any location is proportional to the local bottom slope h_x, the product of the two deep-water tidal velocities, the deep-water depth h_0, and a complicated expression involving A_i. Note that Eq. (10) can also be written as a function of the local tidal velocities and depth using continuity (2). The ratio of the modulation to the mean flow predicted by the model is

$$R = \frac{|\Delta v|}{\bar{v}}, \quad (11)$$

where $|\Delta v|$ nd $\bar{v}$ are given by (10) and (8), respectively.

The functional form of $|\Delta v|$ in (10) is the same as that obtained by squaring a tidal current consisting of two components at frequencies σ_1 and σ_2,

$$|u|^2 = |u_1|^2 + |u_2|^2 + 2|u_1||u_2| \times \cos(\Delta\sigma t + \phi) + \cdots, \quad (12)$$

where u_1 and u_2 are the respective tidal velocities, the cosine term represents the spring–neap modulation at frequency $\Delta\sigma = \sigma_1 - \sigma_2$ and higher frequency terms are neglected. Thus, the envelope of the squared tidal velocity should be coherent with the observed along-bank current at the fortnightly and monthly periods. One way to estimate the amplitude of the mean along-bank flow due to tidal rectification is to estimate the amplitude of the modulation at fortnightly and monthly periods and use the tidal modulation ratio R given by (11) to determine the mean flow. Note that the modulation ratio suggested by (12), namely

$$R_t = \frac{2|u_1||u_2|}{(|u_1|^2 + |u_2|^2)}, \quad (13)$$

is constant in x [by continuity (2)] whereas the ratio given by (11) is not. Therefore, use of R_t to estimate the tidally rectified mean flow is expected to be quantitatively incorrect. We will now apply the model to the southern flank of Georges Bank and attempt to estimate the portion of the mean flow caused by tidal rectification.

3. Data set and model application

Currents were measured at 45 m from August 1976 to June 1978 and at 75 m from August 1976 to March 1979 at station A on the southern flank of Georges Bank (40°51′N, 67°42′W) in water 85 m deep (Fig. 1). The currents were rotated to an along-bank/cross-bank coordinate system (58°–238°, 328°–148°) and low-pass filtered to remove fluctuations having periods shorter than 66 h. Currents were also measured for shorter periods at stations B, C, and D and tidal elevation was measured at stations A and C (Fig. 1). Table 1 summarizes the data and lists the tidal current and elevation amplitudes at each station.

Since the S_2 and N_2 tidal currents on Georges Bank are small compared to the M_2 component, the results of the two-component model discussed above are directly applicable. A transect across the southern flank through Station A from 40 to 2000 m was used for the model topography (Fig. 2). The tidal velocities at 2000 m were estimated from the tidal observations at stations A, B, C, and D (Table 1) using continuity (2). The values were averaged for each tidal constituent. Note that the estimates of the tidal current at 2000 m computed from the mid-depth observations at stations A–D varied by about 8, 26, and 19% for the M_2, N_2, and S_2 constituents, respectively. Corresponding estimates of R_{tN} and R_{tS} varied by 26 and 23%. For all components, especially M_2, the current at 2000 m computed from the observations at station C near the crest of the Bank were smaller than determined at the other stations; this suggests that not all of the cross-bank flow observed at the outer stations goes across the crest of the Bank. The drag coefficient was estimated as $C_D = 0.0015$ from an empirical fit of a bottom boundary layer model to the M2 tidal ellipse profile at station A (P. Daifuku, personal communication, 1982).

The mean along-bank flow $\bar{v}$, the amplitude of the

Unauthenticated | Downloaded 05/27/24 09:13 PM UTC

TABLE 1. Observed amplitude of the bottom pressure (P) and/or tidal currents (U) at M_2 (12.42 h), N_2 (12.66 h), and S_2 (12.00 h) periods at four locations on the southern flank of Georges Bank (Fig. 1). Data pieces are the number of 29 day data records used to calculate the tidal elevation or current, and depth is the depth of the observation. The tidal elevation or current is the mean of the 29 day estimates, and the numbers in parentheses which follow the mean are the standard deviation of the estimates. Bottom pressure is in cm and current is cm s^{-1}. The currents are the amplitude of the major axis of the tidal ellipse; the major axis is typically oriented in the cross-bank direction.

Station Depth (m)	Latitude Longitude	Variable	Pieces	Depth (m)	M_2	N_2	S_2
A	40°51'N	P	14	85	38.9 (±0.3)	9.6 (±0.4)	8.7 (±0.4)
85	67°24'W	U	9	15	36.6 (±2.4)	8.2 (±1.4)	4.7 (±0.8)
			33	45	38.3 (±1.6)	8.5 (±1.2)	5.7 (±0.5)
			33	75	32.5 (±2.0)	6.5 (±1.2)	4.7 (±0.6)
B	40°33'N	U	5	55	11.2 (±1.9)	4.4 (±2.4)	2.2 (±0.8)
250	67°33'W	U	5	200	11.0 (±3.8)	3.3 (±1.0)	2.4 (±1.4)
C	41°03'N	P	12	60	39.8 (±0.5)	9.2 (±0.4)	8.6 (±0.3)
60	67°33'W	U	2	30	55.1 (±0.0)	10.2 (±1.2)	7.2 (±0.6)
D	41°24'N	U	4	15	74.3 (±0.4)	14.8 (±1.1)	9.7 (±0.3)
38	67°34'W						

subtidal modulations $|\Delta v|_S$ and $|\Delta v|_N$, and the modulation ratios R and R_t corresponding to the fortnightly (M_2–S_2) and monthly (M_2–N_2) interactions were computed using the parameters of Table 2 and Eqs. (6)–(11) and (13) (Fig. 2). The S_2 and N_2 components do not significantly increase the mean along-bank flow driven by M_2, but they do cause a significant modulation. At station A, the model predicts a mean along-bank flow of about 1 cm s^{-1} and a modulation of 26 and 44% at 354 and 661 h, respectively. Note that station A is located near a relative minimum of the mean tidally rectified along-bank flow; the model predicts an increased flow off-bank of station A at the shelf break where h_x is large and on-bank of station A where h is small. In the relatively shallow water, the ratios R_S and R_N approach the tidal modulation ratios R_{tS} and R_{tN}, thus suggesting that near the crest of the Bank R_{tS} and R_{tN} (which are easily determined from observation) may be used to estimate the subtidal mean-flow modulation ratios R_S and R_N. This is presumably due to the similar dynamical balance in shallow water for the mean and modulation Eqs. (4) and (9).

The coherence between the envelope of a synthetic surface tide and the observed along-bank flow at station A was used to estimate the amplitude of the modulation of the along-bank flow at fortnightly and monthly periods. A synthetic surface tidal record was created for station A using the observed M_2 (12.42 h period), N_2 (12.66 h period), and S_2 (12.00 h period) constituents. The created tidal record was then squared and low-passed to produce a signal proportional to the envelope of the surface tide squared. The spectra of the observed currents and the coherences between the observed currents and the created tidal envelope were computed using data pieces 3240 h (135 days) long; spectral estimates were obtained at 360 and 648 h which are close to the fortnightly (354 h) and monthly (661 h) periods of interest. Any signal proportional to the envelope of the squared cross-bank tidal-current amplitude could be used for the coherence calculation. A simulated signal was used instead of the observed cross-bank current because energy at the fortnightly and monthly periods of interest may exist in the observed currents which is not due to M_2–N_2 or M_2–S_2 interaction. However, the coherence between the simulated tide and the amplitude of the cross-bank tidal currents squared was 0.99 at both 360 and 648 h. Thus, the results presented here would be only slightly different if the amplitude of the observed cross-bank tidal current squared was used in the analysis, rather than the simulated tide.

4. Mean flow estimate

For periods between 200 and 1000 h, the amplitude of the along-bank current at 45 and 75 m was ~1

TABLE 2. Model parameters used in (6)–(10) to compute the mean flow and the amplitude of the subtidal mean flow modulations shown in Fig. 2.

σ_M	0.000140526 rad s^{-1}
σ_S	0.000145444 rad s^{-1}
σ_N	0.000137862 rad s^{-1}
h_0	2000 m
C_D	0.0015
u_{M0}	0.015 m s^{-1}
u_{N0}	0.0038 m s^{-1}
u_{S0}	0.0024 m s^{-1}
f	0.00009542 rad s^{-1}

Topography:

$$h(x) = \begin{cases} 2602 - 126.8x - 17.81(15 - x)^{1.3}, & 0 < x < 15 \\ 132 - 0.8x + (1.19 \cdot 10^5)(40 - x)^{5.5}, & 15 < x < 40 \\ 132 - 0.8x, & 40 < x < 100 \end{cases}$$

where x is in km and h is in m.

Unauthenticated | Downloaded 05/27/24 09:13 PM UTC

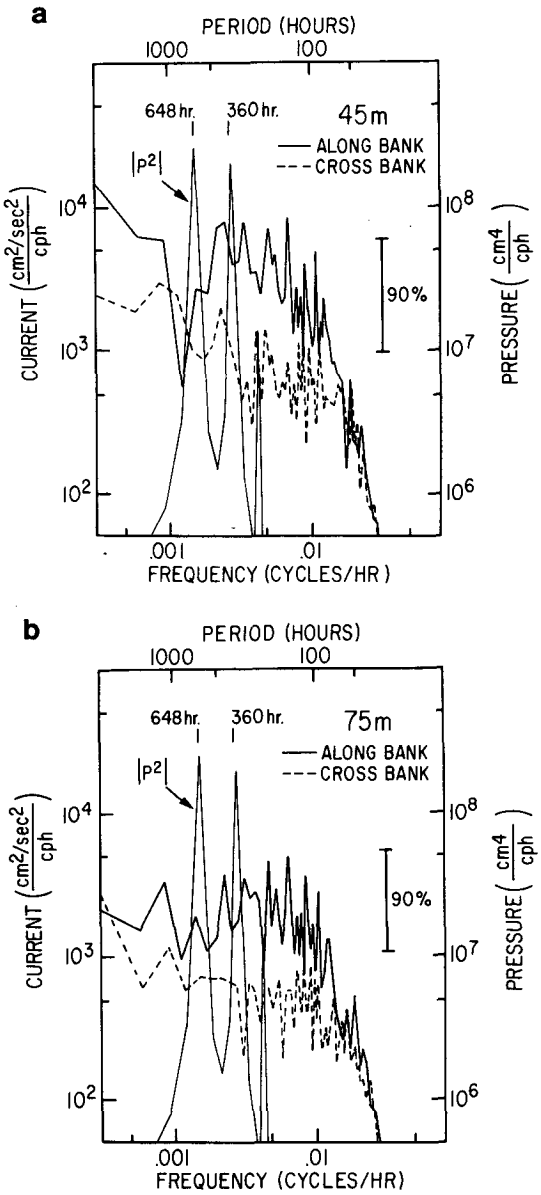

FIG. 3. Autospectra of low-passed currents at station A at (a) 45 m; and (b) 75 m; and the created surface tidal record (squared and low passed). No statistically significant spectral peaks (at 90% confidence level) are present in the current spectra at either 360 or 648 h. Spectra were computed from 5 or 6 pieces (45 and 75 m, respectively) 3240 h (135 days) long.

cm s^{-1}, and no statistically significant spectral peaks (greater than 1 cm s^{-1} above background) were present at either 360 or 648 h (Fig. 3). Of the eight possible coherences between the current and tidal signal that might indicate tidal rectification (two components of current at two depths at two periods), only two were significant at the 90% confidence interval (Fig. 4, Table 3). The along-bank flow at 45 m was marginally coherent (0.68) with the squared tidal signal at 648 h (Fig. 4). In this case, the tidal signal led flow to the northeast by 154° (±45°) and was thus approximately in phase with flow to the southwest as expected for

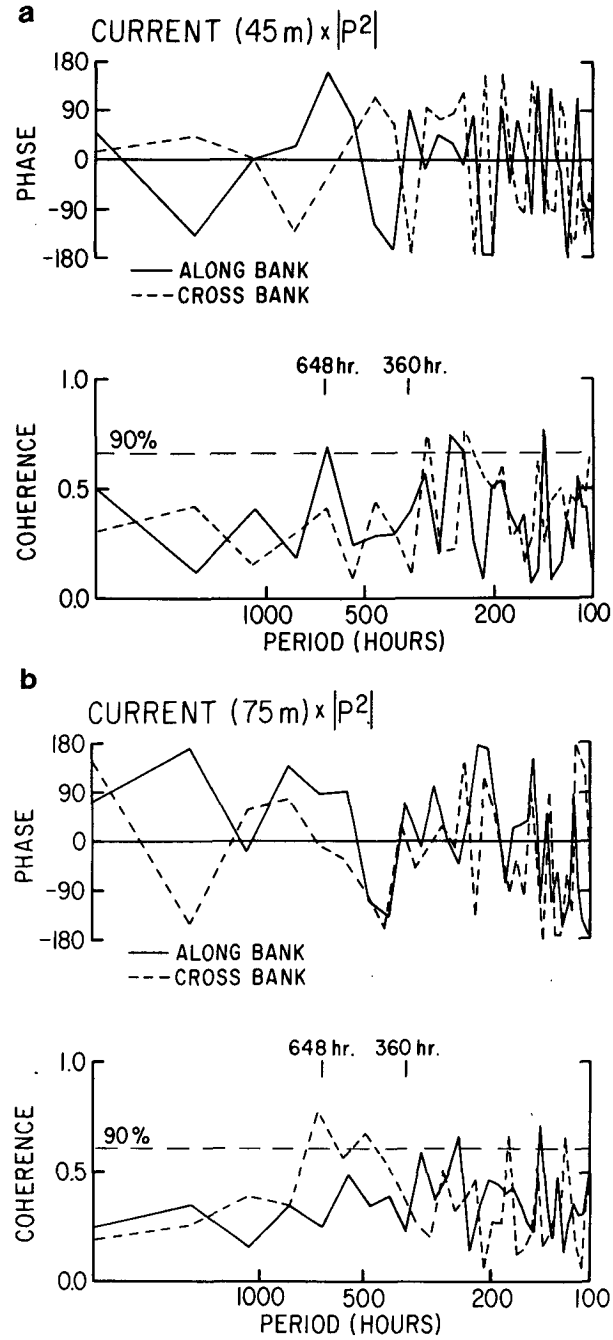

FIG. 4. Coherence between the low-passed squared tidal signal and along-bank and cross-bank flow at (a) 45 m and (b) 75 m. Note that the along-bank flow at 45 m and cross-bank flow at 75 m are marginally coherent with the tidal signal at 648 h. No current components are coherent with the tidal signal at 360 h. Positive phase indicates that current leads pressure. For these figures, positive along-bank current is to the northeast (opposite to model geometry); positive cross-bank flow is toward the northwest (on-bank).

Unauthenticated | Downloaded 05/27/24 09:13 PM UTC

TABLE 3. Variance of the observed along-bank (v) and cross-bank (u) current components at 45 and 75 m at station A at 360 and 648 h, and coherence (coh) between the created tidal signal (squared and low passed) and the current components. Only the underlined coherences are significant. Where the observed coherence is not significant at the 90% confidence level, the coherence is replaced by the significance level in parentheses. Only the along-bank flow at 45 m and the cross-bank flow at 75 m were coherent with the created tide. The modulation of the flow was computed using (15). Positive phase indicates that the simulated pressure leads the current (along-bank positive toward 58°, cross-bank positive toward 328°). Estimates of the upper bound for the mean tidally-rectified current are computed by dividing the modulation estimate by the predicted modulation ratio R in (11). The seasonally adjusted mean current is the observed mean current in winter.

Variable	Depth (m)	Period (h)	Variance ($cm^2\ s^{-2}$)	Coherence	Modulation ($cm\ s^{-1}$)	Phase (°)	Model modulation ratio R	Upper bound mean ($cm\ s^{-1}$)	Seasonally adjusted mean ($cm\ s^{-1}$)
v	45	648	0.84	0.68	0.9	154 (±45)	0.44	2.0	5.5
		360	1.23	(0.67)	<1.1	—	0.24	<4.6	
	75	648	0.59	(0.61)	<0.7	—	0.44	<1.6	3.7
		360	0.48	(0.61)	<0.6	—	0.24	<2.5	
u	45	648	0.31	(0.67)	<0.5				
		360	0.37	(0.67)	<0.6				
	75	648	0.22	0.78	0.5	−8 (±27)			
		360	0.19	(0.61)	<0.4				

tidal rectification. The cross-bank flow at 75 m was also coherent (0.78) and in phase with the tidal signal at 648 h. There was no significant coherence between the tidal signal and the along-bank flow at 75 m and the cross-bank flow at 45 m at 648 h, or between any of the current components and the tidal signal at 360 h.

The observed along-bank current (V) and simulated tide (ST) are modeled as

$$\left.\begin{aligned} V &= \bar{V} + (M_T + N)e^{i2\pi t/T} \\ ST &= \overline{ST} + S_T e^{i2\pi t/T} \end{aligned}\right\},$$

where the overbar denotes the mean, M_T and S_T are modulations at period T (354 or 661 h), and N is noise. Here M_T, S_T, and N are all complex quantities. The squared coherence between V and ST at period T is

$$\gamma_T^2 = \frac{|M_T|^2|S_T|^2}{(M_T + N)^2(S_T)^2},$$

$$= \frac{|M_T|^2}{(M_T + N)^2}. \qquad (14)$$

In (14) N was assumed uncorrelated with M_T and S_T. Since the variance of the along-bank current at period T is

$$a_T^2 = \tfrac{1}{2}(M_T + N)^2.$$

The amplitude of the modulation of the along-bank current was estimated as

$$M_T = (2\gamma_T^2 a_T^2)^{1/2}, \qquad (15)$$

where a_T^2 was determined from the autospectra. When the computed coherence γ_T is less than the 90% confidence limit for zero true coherence (γ_0), the amplitude of the modulation could not be determined from (15). In this case, an upper bound for the modulation amplitude was obtained by defining γ_T to be γ_0; M_T is then the *maximum* current amplitude that *could have been present* in the observed current *without* being statistically coherent with the tidal signal.

The modulations (M_T) computed from (15), the modulation ratios (R) predicted by the model at station A, and the *upper bound* estimates of the tidally rectified mean along-bank flow (M_T/R) are listed in Table 3. (Estimates of cross-bank mean flow are not sensible in the context of the present model.) The observed modulation of the along-bank flow at 648 h was ~0.9 cm s^{-1} at 45 m and was less than 0.7 cm s^{-1} at 75 m. At 360 h the modulation of the along-bank flow was less than 1.1 and 0.6 cm s^{-1} at 45 and 75 m, respectively. In the context of the model presented here, the only significant coherence was between the along-bank flow at 45 m and the simulated tide at 648 h; the amplitude of the modulation was 0.9 cm s^{-1} and thus the estimate of mean tidally rectified along-bank flow was 2.0 cm s^{-1} (using R_N = 0.44). At 75 m, the upper bound was 0.7 cm s^{-1} for the modulation of the along-bank flow at 648 h and thus the mean tidally rectified flow was *less* than 1.6 cm s^{-1}. At 360 h the estimated modulations were 1.1 and 0.6 cm s^{-1} at 45 and 75 m, respectively, which yield upper bounds of 4.6 and 2.5 cm s^{-1} (R_S = 0.24). Thus, the limiting upper bounds were obtained from the modulations at 648 h and were 2.0 cm s^{-1} at 45 m and 1.6 cm s^{-1} at 75 m.

The observed mean current at 45 m varied seasonally. The weakest southwestward flow was in winter, when the cross-bank density gradients were small and was about 5.5 cm s^{-1}. At 75 m there was no seasonal variation of the along-bank flow and the

Unauthenticated | Downloaded 05/27/24 09:13 PM UTC

observed mean current was 3.7 cm s^{-1}. Thus, based on this analysis, ~36% of the mean non-density-driven along-bank flow at 45 m and less than 43% of the mean along-bank flow at 75 m could be attributed to tidal rectification.

5. Discussion

The estimates of the mean along-bank flow caused by tidal rectification at station A on the southern flank of Georges Bank indicate that less than 43% of the mean flow may be due to tidal rectification. These estimates must be viewed with both model assumptions and the limitations of the calculations in mind. Most important, although the amplitude of the modulation of the along-bank flow at monthly and fortnightly periods was estimated from the data, the amplitude of the mean along-bank flow was determined using the ratio of the modulation of the along-bank flow to the mean along-bank flow (12) derived from the analytical model. Quantitatively R may be altered in a more realistic model, as some results are quite sensitive to the choice of model topography. For example, the maximum velocity of the shelf-break jet in Fig. 6c of Loder (1980) is ~9 cm s^{-1} (without the mean-flow interaction) while the maximum velocity of the jet in Fig. 2 is only 3 cm s^{-1}. Also, Loder (personal communication, 1982) repeated his model calculations using topography similar to that examined here and found that the mean-flow interaction has a negligible effect on the mean flow over the outer and mid-shelf region (including station A). This suggests that the results presented for station A should not change on account of mean-flow interaction. Other assumptions, such as along-bank homogeneity and use of the vertically integrated momentum equations, may make the model oversimplified.

The currents at station A were either incoherent or only marginally coherent with the simulated surface tide. Thus, the estimates of the modulation and monthly and fortnightly periods are upper bounds. Since the model modulation $|\Delta v|$ and the squared tidal-signal modulation (as in 12) are of the same functional form, the low coherences could be due to short record length. At 45 and 75 m, the spectral energy was fairly evenly distributed among periods longer than 200 h, implying broad-band processes are forcing currents with amplitudes at ~1 cm s^{-1} at all frequencies. If the full seasonally adjusted current is driven by tidal rectification, the model predicts modulation amplitudes of 1–2 cm s^{-1}, and the currents are expected to be coherent with the simulated tide. However, if only half of the seasonally adjusted mean flow is driven by tidal rectification, even two years of data is apparently marginal to obtain significant coherences at the modulation frequencies.

In addition to the modulation of the along-bank flow at 661 and 354 h caused by tidal rectification, there is an astronomically forced tide at these same periods (Mm and MSf). The major axis of the current for these long period tides should be oriented along-bank. The presence of astronomically forced components could increase or decrease the coherence between the simulated tide and the observed along-bank flow (and thus the estimate of the amplitude of the modulation attributed to tidal rectification) depending on the relative amplitude and phase of the astronomical tide with resect to the spring–neap modulation. Thus, an order-of-magnitude estimate of the Mm and MSf tide is important. The amplitude of the Mm and MSf tidal elevation estimated from the ratio of the astronomical forcing at these long periods to the M_2 forcing (Schureman, 1940) and the observed M_2 tide at station A was 0.9 and 0.8 cm, respectively. Limited tidal constants from Canadian (Yarmouth and Digby, Nova Scotia) and United States coastal stations (Montauk, NY, and Atlantic City, NJ) also indicate Mm and MSf amplitudes of 1–2 cm and a phase of 220° Greenwich in the Gulf of Maine and along the east coast of North America (Canadian Hydrographic Office, 1969; National Ocean Survey, personal communication, 1981). The amplitude of the cross-bank tidal current was estimated from the tidal elevation, assuming that the tide in the Gulf of Maine is co-oscillating, and using continuity. The amplitude of the along-bank current was estimated as f/ω times the cross-bank current, where ω is tidal frequency and f the Coriolis parameter. For a 2 cm tidal elevation, estimated along-bank tidal currents at both Mm and MSf periods were ~0.4 cm s^{-1} and were in phase with the expected along-bank modulation caused by tidal rectification. Although small, the estimated amplitudes of the astronomically forced along-bank currents are of the same order of magnitude as the modulations attributed to tidal rectification (Table 3). The astronomically forced tide was approximately in phase with the expected modulation caused by tidal rectification. Thus, the amplitude of the observed modulations at 661 and 354 h attributed to tidal rectification may be too large by as much as the astronomically forced tidal current. Although the estimates of the amplitude and phase of the Mm and MSf tidal currents are admittedly quite uncertain, this analysis suggests that the estimate of the mean along-bank flow based on the total observed modulation is an upper bound. Note that if the long-period tides had a phase opposite to the tidally rectified flow, the estimate of the mean along-bank flow caused by tidal rectification would be increased by ~1 cm s^{-1}.

Although we sugggest that not all of the observed southwestward flow at station A can be attributed to tidal rectification, the results are not inconsistent with the theory of tidal rectification. In fact, the observations are in agreement with the extended model results. The analytical model predicts a mean along-bank flow of about 1 cm s^{-1} at station A while the

Unauthenticated | Downloaded 05/27/24 09:13 PM UTC

modulation analysis using the analytical model and observation suggests the mean flow was about 2.0 cm s^{-1} or less. The relatively weak along-bank flow at station A attributed to tidal rectification also does not indicate that tidal rectification is unimportant in driving the stronger observed along-bank flow in other regions of Georges Bank. The model suggests that station A is located in a valley of $\bar{v}$ (Fig. 2) and thus the small along-bank flow at station A is consistent with the existence of a stronger jet over the upper slope and toward the crest of the bank. Clearly, station A is not the best location to test for tidal rectification. Estimates of the along-bank flow caused by tidal rectification in these areas where the relative contribution by tidal rectification should be larger would be of interest. However, the mean flow estimation method used here must be applied with care in the region of the jet since R is quite variable. Current observations on the northern flank of the bank indicate that temporal and spatial variations of the along-bank flow may complicate estimates of the tidally rectified flow made from Eulerian measurements (Magnell *et al.,* 1980).

The observed coherence between the created surface tidal signal and the cross-bank flow at 75 m indicates a modulation of the cross-bank flow of ~0.5 cm s^{-1} in phase with the surface tide at 648 h. The Eulerian cross-bank flow associated with tidal rectification was not discussed in detail by Loder and is not considered here. However, some cross-bank circulation may be expected and could have important implications for the transport of material on or off Georges Bank.

Several other mechanisms may also contribute to the observed mean along-bank flow on the southern flank of the Bank. An along-bank pressure gradient may partially drive the southwestward flow; such a gradient has been suggested as a mechanism to drive the mean flow in the Middle Atlantic Bight (Csanady, 1976; Beardsley and Boicourt, 1981). In addition, wind stress and cross-bank and along-bank density gradients may be important. The three-dimensional nature of these effects is likely to require numerical solutions to determine quantitatively the relative importance of tidal rectification in the observed around-bank flow on Georges Bank.

Acknowledgments. J. Moody calculated the tidal constituents for the data records listed in Table 1 and created the surface tidal record. We also acknowledge constructive comments from John Loder and an anonymous reviewer. Support for this work was provided to B. Butman and M. Noble by the U.S. Geological Survey and by the U.S. Bureau of Land Management under Interagency Agreement AA851-IA1-17 and Memoranda of Understanding AA551-MU0-18, AA551-MU9-4, AA551-MU8-21, AA550-MU7-31, and AA550-MU5-33; to R. C. Beardsley by the National Science Foundation under OCE80-14941; and to D. C. Chapman by a postdoctoral fellowship from the Woods Hole Oceanographic Institution.

REFERENCES

Beardsley, R. C., and W. C. Boicourt, 1981: On estuarine and continental shelf circulation in the Middle Atlantic Bight. *Evolution of Physical Oceanography,* B. A. Warren and C. Wunsch, Eds., MIT Press, 198–233.

Butman, B., R. C. Beardsley, B. Magnell, D. Frye, J. A. Vermersch, R. Schlitz, R. Limeburner, W. R. Wright and M. A. Noble, 1982: Recent observations of the mean circulation on Georges Bank. *J. Phys. Oceanogr.,* **12,** 569–591.

Canadian Hydrographic Office, 1969: *Harmonic Constants and Associated Data from Canadian Tidal Water.* Vol. 1, Atlantic Coast, Tides and Water Level Marine Science Branch, Dept. Energy, Mines and Resources, Ottawa, Canada.

Csanady, G. T., 1976: Mean circulation in shallow seas. *J. Geophys. Res.,* **81,** 5389–5399.

Hopkins, T. S., and N. Garfield III, 1981: Physical origins of Georges Bank water. *J. Mar. Res.,* **39,** 465–500.

Hunter, J. R., 1975: A note on quadratic friction in the presence of tides. *Estuarine Coastal Mar. Sci.,* **3,** 473–475.

Huthnance, J. M., 1973: Tidal current asymmetries over the Norfolk Sandbanks. *Estuarine Coastal Mar. Sci.,* **1,** 89–99.

Loder, J., 1980: Topographic rectification of tidal currents on the sides of Georges Bank. *J. Phys. Oceanogr.,* **10,** 1399–1416.

Magnell, B. A., S. L. Spiegel, R. I. Scarlet and J. B. Andrews, 1980: The relationship of tidal and low-frequency currents on the north slope of Georges Bank. *J. Phys. Oceanogr.,* **10,** 1200–1212.

Schureman, P., 1940: *Manual of Harmonic Analysis and Prediction of Tides.* U.S. Dept. Commerce, Coast and Geodetic Survey Special Publication 98, U.S. Government Printing Office, Washington, D.C., 317 pp.

Unauthenticated | Downloaded 05/27/24 09:13 PM UTC